A&A 417, 1183–1188 (2004)
DOI: 10.1051/0004-6361:20034197

Astronomy & Astrophysics

Dielectronic recombination data for dynamic finite-density plasmas

V: The lithium isoelectronic sequence

J. Colgan[1], M. S. Pindzola[1], and N. R. Badnell[2]

[1] Department of Physics, Auburn University, Auburn, AL, 36849, USA
[2] Department of Physics, University of Strathclyde, Glasgow, G4 0NG, UK

Received 14 August 2003 / Accepted 2 October 2003

Abstract. Dielectronic recombination data for the lithium isoelectronic sequence has been calculated as part of the assembly of a dielectronic recombination database necessary for modelling of dynamic finite-density plasmas (Badnell et al. 2003). Dielectronic recombination coefficients for a selection of ions from this sequence are presented and the results discussed.

Key words. atomic data – atomic processes – plasmas

1. Introduction

The programme to generate a total and final state level-resolved intermediate coupling dielectronic recombination database necessary for spectroscopic modelling of dynamic finite-density plasmas, where the coronal approximation is not valid, has been described by Badnell et al. (2003). To this end, work has been underway in calculations of dielectronic recombination data for the oxygen, carbon (Zatsarinny et al. 2003, 2004) and beryllium (Colgan et al. 2003) isoelectronic sequences. In this paper we describe calculations and results for dielectronic recombination data for the lithium isoelectronic sequence. This sequence has shown to be important in the astrophysical modelling of the intergalactic medium abundance ratio (Savin 2000). Although many studies of this sequence have been made, most of these present only total recombination rates from the ground state. Here we present total and partial recombination rates from ground and excited states.

There have been numerous studies of dielectronic recombination for many of the ions in the lithium isoelectronic sequence. The first experimental measurements for lithium-like ions were made by Dittner et al. (1987) on B^{2+}, C^{3+}, N^{4+}, and O^{5+} using a single-pass merged beams method with a very broad experimental resolution. These measurements were generally in good agreement with configuration-average distorted-wave dielectronic recombination calculations of B^{2+}, C^{3+}, and O^{5+} made by Griffin et al. (1985). The configuration-average cross sections were found to be in approximate agreement with intermediate-coupling calculations, but were a factor of 3/2 larger than *LS*-coupling calculations. This reduction factor of 2/3 for s → p dielectronic recombination cross sections in pure *LS*-coupling was first pointed out by Trefftz (1969). The configuration-average calculations were later extended to include both intermediate-coupling and electric field enhancement effects (Griffin et al. 1985, 1987) for lithium-like ions from B^{2+} to Fe^{23+}.

In 1990 experimental measurements were reported by Andersen et al. (1990) on C^{3+} and O^{5+} at much narrower energy resolution. It was found that the agreement between theory and experiment was very good for low n configurations and that the inclusion of electric field effects within an intermediate coupling calculation was necessary for theoretical calculations to obtain agreement with these measurements for high n configurations (Griffin et al. 1989). Similar results were obtained for N^{4+}, F^{6+}, and Si^{11+}, by Andersen et al. (1992). Chen (1991) calculated the total dielectronic recombination rate coefficients for 11 ions in the lithium isoelectronic sequence using distorted-wave techniques in a multiconfiguration Dirac-Fock model. Other intermediate-coupling calculations of dielectronic recombination rate coefficients for Be^{+} and B^{2+} were made by Pindzola & Badnell (1992). Both these sets of calculations were fitted by Mazzotta et al. (1998) and tabulated in their study of the ionization equilibrium for a range of atoms and ions.

Some of the first storage ring experiments made at the TSR ring in Heidelberg, Germany, were shown to be in good agreement with intermediate-coupling AUTOSTRUCTURE calculations of dielectronic recombination cross sections of Cu^{26+} (Kilgus et al. 1992). The cooler electrons employed in this technique allowed resolution of resonances associated

Send offprint requests to: J. Colgan,
e-mail: jcolgan@physics.auburn.edu

with $\Delta n = 0$ and $\Delta n = 1$ excitations and some resolution of fine structure components. This good agreement between theory and experiment was extended to Ar^{15+} by Schennach et al. (1994).

Calculations by Gorczyca et al. (1996) on dielectronic recombination cross sections of Ar^{15+} included *R*-matrix dielectronic recombination calculations, which were in good agreement with the intermediate-coupling AUTOSTRUCTURE calculations. These accurate close-coupling calculations were able to investigate the effects of interference between dielectronic recombination and radiative recombination (the independent processes approximation) and also the interference between the dielectronic recombination resonances themselves. It was found that the overall effect of interference between the dielectronic recombination and the background radiative recombination for the total rate coefficient was quite small. Further studies of Ar^{15+} were also made by Zong et al. (1997) who made an accurate measurement of the $\Delta n = 0$ dielectronic recombination resonances. It was found that, in order to get good agreement with the experimental measurements of the positions and widths of the doubly excited states of Ar^{15+}, fully relativistic perturbation theory calculations were necessary which included radiative corrections and mass polarization terms.

In the late 1990's the effects of electric fields on the dielectronic recombination cross section were further investigated using the heavy ion storage ring CRYRING in Stockholm. These high resolution experiments revealed discrepancies with earlier calculations for Si^{11+} (Bartsch et al. 1997). This was partly due to the increased precision of the experiments which now allowed resolution of individual *nl* states within each *n*-manifold. The position of these states was also very sensitive to configuration-interaction effects and also enhancement effects of crossed electric and magnetic fields. Extended calculations (Griffin et al. 1998) which now included the effects of crossed electric and magnetic fields within the intermediate-coupling calculations went some way to matching the experimental results. The influence of electromagnetic fields on dielectronic recombination of O^{5+} was also studied jointly by experiment and theory by Böhm et al. (2002, 2003). Noticeable enhancement of the dielectronic recombination cross section as a function of the field strength was observed, although quantitative discrepancies remained between experiment and theory. Further calculations which included the interaction between resonances in the enhancement of dielectronic recombination by an electric field were made on C^{3+}, Ne^{7+}, and Si^{11+} (Griffin et al. 1998). The interference between dielectronic recombination and the background radiative recombination was further explored by Mitnik et al. (1999) for F^{6+}, in both the final state level-resolved and total recombination rates.

Recent very high resolution experiments using the CRYRING facility have been made, also on C^{3+} for low collision energies (Mannervik et al. 1998). These high-precision measurements have mapped out peaks in the dielectronic recombination spectra corresponding to the individual *nl* resonances. The theoretical calculations required to reproduce these experimental measurements prove very challenging. Extensive configuration-interaction and QED effects must be included in any calculation in order to accurately determine the position of the *nl* resonances. Another high-resolution measurement of the dielectronic recombination rate coefficient associated with $\Delta n = 0$ excitations in C^{3+} has been made recently by Schippers et al. (2001) at the TSR in Heidelberg. A total dielectronic and radiative recombination rate coefficient was quoted to within a systematic uncertainty of 15%. Further high resolution measurements were also made by this group in their study of $\Delta n = 0$ excitations in Ni^{25+} (Schippers et al. 2000). The influence of external electric and magnetic fields was also assessed. More high-resolution CRYRING measurements were made on N^{4+} by Glans et al. (2001) and F^{6+} by Tokman et al. (2002), in the energy range up to around 1 eV above threshold. The latter set of experiments show the need for fully relativistic calculations incorporating QED effects are necessary to accurately map out the experimentally resolved resonances.

In this paper we describe the calculations made of dielectronic recombination final state level-resolved rate coefficients for the lithium-like isoelectronic sequence for all ions up to Ar^{15+} as well as Ca^{17+}, Ti^{19+}, Cr^{21+}, Fe^{23+}, Ni^{25+}, Zn^{27+}, Kr^{33+}, Mo^{39+}, and Xe^{51+}. It would clearly be impractical to list rate coefficients for all these ions in a paper publication. As previously discussed (Badnell et al. 2003), this data will form part of an Atomic Data and Analysis Structure (ADAS) dataset comprising the *adf09* files for each ion, detailing the rate coefficients to each *LS* and *LS J*-resolved final state. This is available through the ADAS project (Summers 2001) and is also made available online at the Oak Ridge Controlled Fusion Atomic Data Center.

These calculations attempt to produce dielectronic recombination final state level-resolved coefficients over a wide range of temperatures and atomic ions. Consequently, in some respects, our data will not be as accurate as more detailed calculations described previously, since we do not include any electric or magnetic field effects that may affect the dielectronic recombination coefficients in a plasma (Griffin et al. 1985, 1998). However, it was found by Badnell et al. (1993) that the apparent large enhancement of zero density dielectronic recombination rates by the plasma micro field was in fact partially cancelled by ionization from excited states. In addition, the effects of interacting resonances, or the effects of dielectronic recombination/radiative recombination interference, while unlikely to affect the total recombination rate, may affect the final state level-resolved rate coefficients. However, the rate coefficients detailed here do cover a wide range of temperatures and ionic species, and are expected to be broadly accurate in most respects. Our intermediate-coupling calculations are expected to be the most accurate, although we present *LS*-coupled calculations as well for comparison. In Sect. 2 we give a brief description of the theory used and the details of our calculations for the lithium like ions. In Sect. 3 we present results for dielectronic recombination rate coefficients for selected ions in this sequence. We conclude with a brief summary.

2. Theory

The theoretical details of our calculations have already been described in detail (Badnell et al. 2003). Here we outline only

the main points. The AUTOSTRUCTURE code (Badnell 1986, 1997; Badnell & Pindzola 1989) is used to calculate configuration mixing *LS* and intermediate-coupling energy levels, radiative, and autoionization rates. The autoionization rates are calculated in the isolated resonance approximation using distorted waves. The enables the generation of final state level-resolved and total dielectronic recombination rate coefficients in the independent processes approximation, i.e. we neglect interference between the radiative recombination and the dielectronic recombination rate, which has been found to be a small effect for most of the partial rates (Pindzola et al. 1992).

The dielectronic recombination process for lithium-like ions can be represented, in intermediate coupling, for $\Delta n = 0$ excitation, by

$$1s^2 2s[^2S_{1/2}] + e^- \rightarrow 1s^2 2p[^2P_{1/2,3/2}]nl, \quad (1)$$

which can radiatively decay emitting a photon when either the 2p electron drops back into the 2s subshell or when the nl electron drops into a lower $n'l'$ shell which is bound. In Eq. (1) l and n values were included up to 15 and an approximation for high-level values of n up to 1000 was used (Badnell et al. 2003). For $\Delta n = 1$ excitation from the $n = 2$ shell, the dielectronic recombination processes can be written as

$$\begin{aligned} 1s^2 2s[^2S_{1/2}] + e^- &\rightarrow 1s^2 3l[^2L_J]nl', \\ 1s^2 2p[^2P_{1/2,3/2}] + e^- &\rightarrow 1s^2 3l[^2L_J]nl', \end{aligned} \quad (2)$$

which can radiatively decay emitting a photon when either the $3l$ or nl' electron drops back into a lower subshell. We also include $\Delta n = 1$ excitation processes from the $n = 1$ shell, namely

$$\begin{aligned} 1s^2 2s[^2S_{1/2}] + e^- &\rightarrow 1s2s^2[^2S_{1/2}]nl', \\ 1s^2 2p[^2P_{1/2,3/2}] + e^- &\rightarrow 1s2s2p[^4P_J\ ;\ ^2P_J]nl', \end{aligned} \quad (3)$$

which again can radiatively decay emitting a photon when a $2l$ or nl' electron drops into a lower subshell. In addition, we include the core re-arrangement decay to $1s^2nl' + e^-$. Values of l' up to $l' = 6$ were included along with values of n up to $n = 15$ for both $\Delta n = 1$ transitions. Again an approximation for the high-level values of n was used up to $n = 1000$. AUTOSTRUCTURE is implemented within the ADAS suite of programs as ADAS701. It produces raw autoionization and radiative rates which must be post-processed to obtain the final state level-resolved and total dielectronic recombination rates. The post-processor ADASDR is used to reorganize the resultant data and also to add in radiative transitions between highly-excited Rydberg states, which are computed hydrogenically. This post-processor outputs directly the *adf09* file necessary for use by ADAS. Separate files are produced for the different core excitations. For the lithium isoelectronic sequence we calculate dielectronic recombination rate coefficients for the $\Delta n = 0$ and $\Delta n = 1$ transitions and so, generally, six *adf09* files are produced since we calculate in both the *LS* and intermediate-coupling configuration mixed approximations.

3. Results

The *adf09* files generated by our calculations in both the *LS* and intermediate-coupling configuration mixed approximations, for both the $\Delta n = 0$ and $\Delta n = 1$ transitions are available on the www (`http://www-cfadc.phy.ornl.gov`). They provide final state level-resolved dielectronic recombination rate coefficients into final *LS* terms or *LS J* levels in a manner useful to fusion and astrophysical modellers. All of our total intermediate-coupling rate calculations were also fitted with the following formula

$$\alpha = \frac{1}{T^{3/2}} \sum_{i=1}^{5} c_i e^{-E_i/T}, \quad (4)$$

to facilitate comparison with other work. In this equation T and E_i have units of Kelvin and the rate coefficients α have units cm^3 s^{-1}. Our fits are accurate to better than 3%, for all ions in the temperature range $Z^2(5 \times 10^3 - 1 \times 10^7)$ K, where Z is the residual charge of the initial ion. In Table 1 we present a list of the coefficients c_i and E_i for each member of the lithium isoelectronic sequence. In these fitting coefficients the $\Delta n = 0$ and $\Delta n = 1$ transitions have been added together. We also plot some examples of the final state level-resolved and total rate coefficients that are derived from the *adf09* files for several atomic ions in the lithium-like sequence.

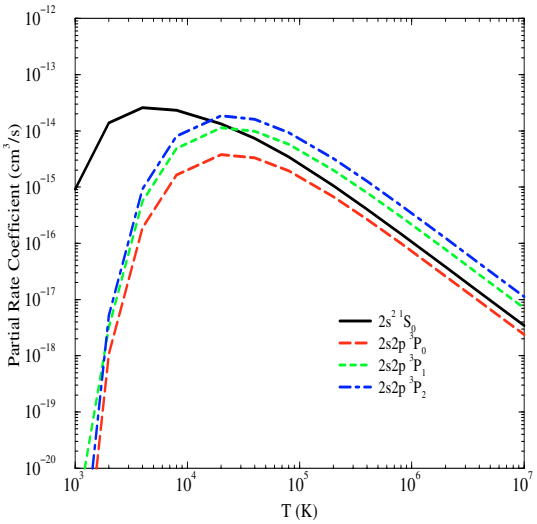

Fig. 1. Dielectronic recombination final state level-resolved rate coefficient for B^{2+} as a function of electron temperature (in Kelvin). We present final state level-resolved rate coefficients from the initial $1s^2 2s\ ^2S_{1/2}$ level to the final state levels as indicated (where we have dropped the $1s^2$ part of the configuration for clarity).

As an example of the final state level-resolved rate coefficients available, we present in Fig. 1 final state level-resolved dielectronic recombination rate coefficients for B^{2+}, calculated within the intermediate-coupling approximation. The rate coefficients are from the initial $1s^2 2s\ ^2S_{1/2}$ level to the final state levels $1s^2 2s^2\ ^1S_0$, $1s^2 2s2p\ ^3P_0$, $1s^2 2s2p\ ^3P_1$, and $1s^2 2s2p\ ^3P_2$, as indicated on the figure. Of course there exists hundreds of final state levels, for this ion alone, for which the dielectronic recombination final state level-resolved rate coefficients are tabulated in the *adf09* files; here we only plot several examples as an illustration of the data. It is clear that at low temperatures, as expected, the ion recombines preferentially into the $1s^2 2s^2\ ^1S_0$ level due to its lower energy.

In Fig. 2 we show the total dielectronic recombination rate coefficient for both Be^+ and B^{2+}. In both cases we compare

Table 1. Fitting coefficients c_i and E_i for Eq. (5), for ions in the lithium isoelectronic sequence. All coefficients refer to our intermediate-coupling calculations.

Ion	c1	c2	c3	c4	c5	E1	E2	E3	E4	E5
Be^{+}	2.228(−5)	7.121(−4)	···	···	···	2.954(+4)	4.661(+4)	···	···	···
B^{2+}	1.844(−5)	1.908(−3)	4.113(−5)	···	···	2.451(+4)	6.228(+4)	2.320(+5)	···	···
C^{3+}	2.556(−5)	2.222(−3)	1.076(−3)	1.635(−4)	2.500(−3)	3.329(+3)	8.181(+4)	1.216(+5)	6.096(+5)	3.295(+6)
N^{4+}	9.033(−5)	4.470(−3)	8.358(−4)	2.673(−3)	2.557(−3)	1.462(+4)	1.106(+5)	4.548(+5)	4.077(+6)	5.355(+6)
O^{5+}	3.966(−4)	5.938(−3)	2.352(−3)	9.375(−3)	4.261(−3)	4.611(+4)	1.416(+5)	8.650(+5)	6.112(+6)	6.112(+6)
F^{6+}	2.256(−4)	3.383(−3)	4.733(−3)	4.693(−3)	2.466(−2)	3.859(+3)	1.142(+5)	2.047(+5)	1.156(+6)	7.801(+6)
Ne^{7+}	5.522(−4)	9.024(−3)	8.840(−3)	2.227(−3)	3.948(−2)	3.511(+4)	1.769(+5)	1.212(+6)	3.056(+6)	9.773(+6)
Na^{8+}	5.171(−4)	1.080(−2)	1.521(−2)	5.886(−3)	5.782(−2)	3.847(+3)	1.840(+5)	1.491(+6)	5.308(+6)	1.208(+7)
Mg^{9+}	1.196(−3)	1.258(−2)	2.704(−2)	9.530(−3)	8.006(−2)	4.518(+4)	2.235(+5)	2.002(+6)	8.368(+6)	1.441(+7)
Al^{10+}	8.730(−4)	4.099(−3)	1.200(−2)	3.935(−2)	1.154(−1)	9.548(+3)	1.223(+5)	2.938(+5)	2.508(+6)	1.617(+7)
Si^{11+}	1.737(−3)	1.583(−2)	9.831(−3)	5.245(−2)	1.437(−1)	5.679(+4)	2.523(+5)	1.549(+6)	3.245(+6)	1.888(+7)
P^{12+}	2.544(−3)	1.912(−2)	7.313(−2)	2.948(−2)	1.516(−1)	3.947(+4)	2.864(+5)	3.200(+6)	1.265(+7)	2.291(+7)
S^{13+}	2.767(−3)	2.221(−2)	9.530(−2)	5.194(−2)	1.619(−1)	2.881(+4)	3.032(+5)	3.687(+6)	1.681(+7)	2.660(+7)
Cl^{14+}	4.330(−3)	1.733(−2)	1.199(−1)	1.675(−1)	5.092(−2)	9.792(+4)	4.106(+5)	4.305(+6)	2.499(+7)	3.774(+7)
Ar^{15+}	2.929(−2)	1.507(−1)	1.049(−1)	1.086(−1)	7.082(−2)	2.446(+5)	4.506(+6)	2.958(+7)	2.958(+7)	2.958(+7)
Ca^{17+}	6.404(−3)	3.502(−2)	2.084(−1)	3.362(−1)	1.823(−1)	3.796(+4)	3.975(+5)	5.759(+6)	3.506(+7)	8.737(+7)
Ti^{19+}	1.675(−2)	3.693(−2)	2.841(−1)	2.664(−1)	1.560(−1)	1.463(+5)	6.311(+5)	7.186(+6)	3.922(+7)	5.568(+7)
Cr^{21+}	9.821(−3)	4.792(−2)	4.511(−2)	3.380(−1)	4.694(−1)	6.706(+4)	4.471(+5)	3.528(+6)	9.553(+6)	5.460(+7)
Fe^{23+}	1.319(−2)	5.592(−2)	4.275(−2)	4.212(−1)	5.356(−1)	7.897(+4)	4.942(+5)	3.272(+6)	1.089(+7)	6.441(+7)
Ni^{25+}	1.743(−2)	7.232(−2)	1.884(−1)	3.781(−1)	5.618(−2)	6.560(+4)	5.778(+5)	7.056(+6)	1.565(+7)	7.704(+7)
Zn^{27+}	1.892(−2)	7.764(−2)	6.135(−2)	5.804(−1)	6.481(−2)	6.620(+4)	5.557(+5)	3.394(+6)	1.392(+7)	8.379(+7)
Kr^{33+}	4.371(−2)	1.392(−1)	5.006(−1)	4.672(−1)	6.978(−1)	1.592(+5)	1.037(+6)	1.285(+7)	3.121(+7)	1.315(+8)
Mo^{39+}	5.184(−2)	1.860(−1)	2.248(−1)	9.836(−1)	8.282(−1)	4.426(+4)	9.383(+5)	6.410(+6)	2.797(+7)	1.729(+8)
Xe^{51+}	1.289(−1)	3.569(−1)	4.323(−1)	1.173(+0)	9.400(−1)	5.127(+5)	2.477(+6)	1.196(+7)	4.604(+7)	2.898(+8)

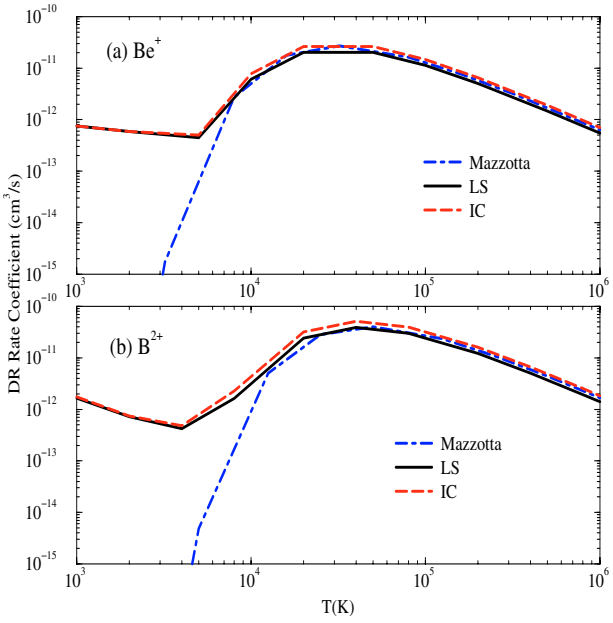

Fig. 2. Dielectronic recombination rate coefficient for **a)** Be^{+} and **b)** B^{2+} as a function of electron temperature (in Kelvin). We compare our calculations using *LS* configuration mixing and intermediate-coupling configuration mixing with data from the fitted coefficients of Mazzotta et al. (1998).

our *LS* and intermediate-coupling data with results fitted from the tables of Mazzotta et al. (1998), where, for these two ions they adopted the dielectronic recombination calculations of Pindzola & Badnell (1992). In this figure, we have added together the contributions to the rate coefficient from the $\Delta n = 0$ and $\Delta n = 1$ transitions. The agreement between our two calculations and Mazzotta et al. (1998) is very good down to around 10^4 K, where below this temperature, the fit of Mazzotta et al. (1998) is an extrapolation.

In Fig. 3 we present partial dielectronic recombination rate coefficients for C^{3+} for only the $\Delta n = 0$ transition, over a wide range of electron temperature. As previously discussed, the dielectronic recombination for this ion has been the subject of many theoretical and experimental investigations (see Savin 2000 for a review). Here we compare with two recent fits: those of Mazzotta et al. (1998) and a fit to the experimental results of Schippers et al. (2001). The fits of Mazzotta et al. (1998) were from the calculations of Chen (1991). Our results are in good agreement at higher temperatures, but are in major disagreement at temperatures below 10^5 K. Chen (1991) presented data only from 10^5 K upwards and it seems likely that the fits of Mazzotta et al. (1998) become inaccurate at very low temperatures. Above 10^5 K our results are in very good agreement, which is to be expected since the calculations of Chen (1991) are very similar to ours. In the lower temperature range our results are in good agreement with the fit of Schippers et al. (2001), especially our intermediate-coupling calculations. Schippers et al. (2001) quote a systematic uncertainty of 15% in their measurements. We note that our *LS* calculations are lower than the intermediate-coupling rate coefficients and those of Schipper et al. (2001) by approximately a factor of 2/3, in accord with the previous discussion. We remark here also that, with regard to the discussion of a factor of 2 scatter between theoretical calculations for dielectronic recombination of C^{3+}

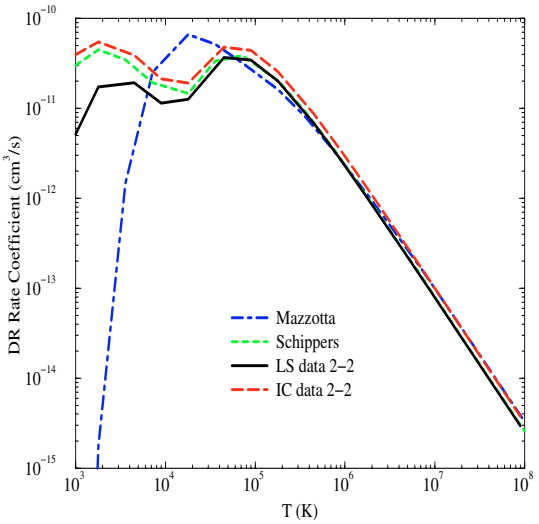

Fig. 3. Dielectronic recombination rate coefficient for C^{3+} as a function of electron temperature (in Kelvin), for the $\Delta n = 0$ transition only. Again the *LS* and intermediate-coupling data are compared with data from the fitted coefficients of Mazzotta et al. (1998). We also compare with the recent fit of Schippers et al. (2001) for which they quote a systematic uncertainty of around 15%.

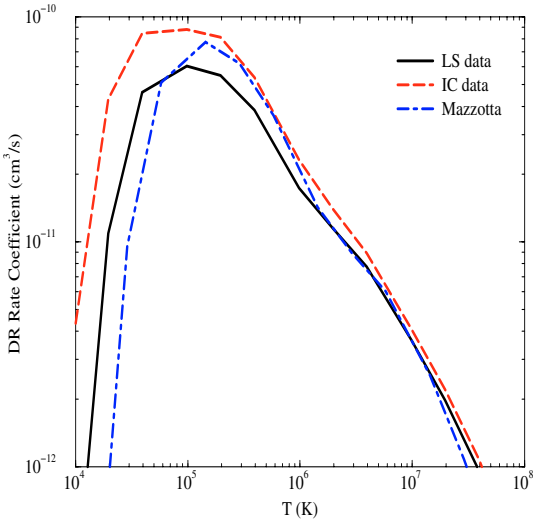

Fig. 4. Dielectronic recombination rate coefficient for Cl^{14+} as a function of electron temperature (in Kelvin). Again the *LS* and intermediate-coupling data are compared with data from the fitted coefficients of Mazzotta et al. (1998).

by Savin (2000), our calculations are in good agreement with the IC calculations of Badnell quoted by Savin (2000) for the temperature range considered here.

In Fig. 4 we again compare our total dielectronic recombination rate coefficients with those of Mazzotta et al. (1998), this time for the dielectronic recombination of Cl^{14+}. Again at high temperature there is reasonable agreement between the three calculations. At low temperature (in this case below 10^5 K) there are major differences between our calculations and those of Mazzotta et al. (1998). Again the data of Chen (1991) was presented only for temperatures above 10^5 K, below which the fits of Mazzotta et al. (1998) seems to become inaccurate. Also

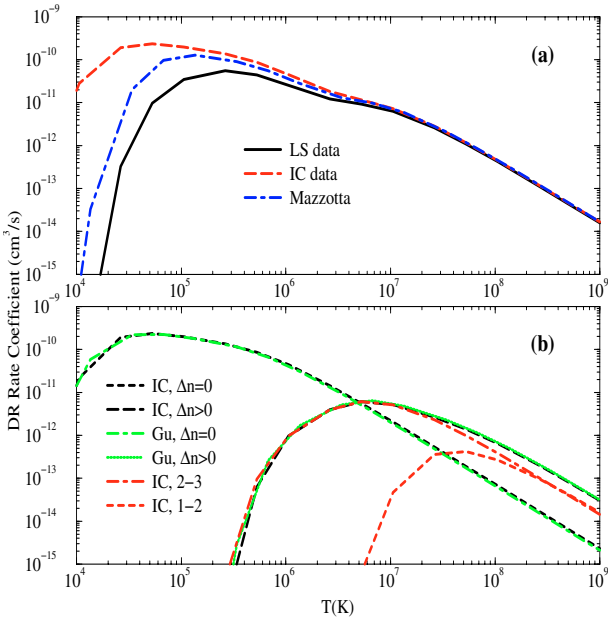

Fig. 5. Dielectronic recombination rate coefficients for Fe^{23+} as a function of electron temperature (in Kelvin). In **a)** we compare our *LS* and intermediate-coupling data the fitted coefficients of Mazzotta et al. (1998). In **b)** we compare our intermediate-coupling calculations with the calculations of Gu (2003). We compare the $\Delta n = 0$ and $\Delta n \geq 0$ transitions separately. We also show the intermediate-coupling contributions to the $\Delta n \geq 0$ sum from the $n = 2-3$ and $n = 1-2$ transitions.

in this range the *LS* and intermediate-coupling calculations begin to differ significantly.

Finally, in Fig. 5 we present total dielectronic recombination rate coefficients for Fe^{23+}. In (a) we compare our *LS* and intermediate-coupling calculations with those of Mazzotta et al. (1998), which were based on the calculations of Chen (1991). We see again good agreement between our calculations and those of Mazzotta et al. (1991) at high temperature. At low temperature there are again differences between the calculations, for the same reasons as mentioned previously. For this quite high-Z ion the *LS* calculations are considerably lower than the intermediate-coupling calculations.

In Fig. 5b we can compare our calculations with the very recent calculations of Gu (2003). He used a fully relativistic distorted-wave method to calculate dielectronic recombination rate coefficients for selected ions of astrophysical interest. In Fig. 5b we compare our rate coefficients for Fe^{23+} for the separate contributions from the $\Delta n = 0$ and $\Delta n > 0$ transitions. The agreement between the present calculations and those of Gu (2003) is excellent over the entire temperature range. We note however that, in order to compare as closely as possible with the calculations of Gu (2003), it is necessary to include the contribution to the rate coefficient from inner shell transitions, i.e., from the 1s shell. As seen in Fig. 5b from the individual contributions to the $\Delta n > 0$ transition, this is quite a small effect which only is important at the highest temperatures considered here. This agreement applies not only to Fe^{23+} but extends to the other lithium-like ions with which it is possible to compare, which are not shown here.

4. Summary

In this paper we have described calculations of dielectronic recombination data for the lithium-like isoelectronic sequence as part of an assembly of a dielectronic recombination database necessary for the modelling of dynamic finite-density plasmas (Badnell et al. 2003). We have calculated LSJ final state level-resolved dielectronic recombination rate coefficients in a form which will prove of great use to astrophysical and fusion plasma modellers. Although our approximations are such that each final state level-resolved dielectronic recombination rate coefficient may not be as highly accurate as some of the most sophisticated techniques available today, we have calculated our data over a wide temperature range and for a large number of atomic ions in order to maximise the available information for modelling work.

We have presented selected final state level-resolved and total rate coefficients for some ions of interest and have made comparisons, where possible, with previous work. In the high temperature range we have found good agreement with the calculations of Chen (1991), which have been fitted by Mazzotta et al. (1998). However, it appears that the fits of Mazzotta et al. (1998) may become inaccurate in the low temperature range. For C^{3+} we have found good agreement with the published fitted coefficients to the measurements of Schippers et al. (2001), over a wide range of temperatures, down to 10^3 K. For Ni^{25+} our calculations are also in very good agreement with the measurements of Schippers et al. (2000) in the range 2−100 eV, although this comparison is not shown here. Our calculations are also in very good agreement with the recent work of Gu (2003) for the ions with which it is possible to compare. Our fits are accurate to better than 3%, for all ions in the temperature range $Z^2(5 \times 10^3 - 1 \times 10^7)$ K, where Z is the residual charge of the initial ion. In the future we will present dielectronic recombination data for further isoelectronic sequences as detailed previously (Badnell et al. 2003).

Acknowledgements. This work was supported in part by the US Department of Energy. Computational work was carried out at the National Energy Research Scientific Computing Center in Oakland, CA.

References

Andersen, L. H., Bolko, J., & Kvistgaard, P. 1990, Phys. Rev. A, 41, 1293
Andersen, L. H., Pan, G. Y., Schmidt, H. T., Pindzola, M. S., & Badnell, N. R. 1992, Phys. Rev. A, 45, 6332
Badnell, N. R. 1986, J. Phys. B, 19, 3827
Badnell, N. R. 1997, J. Phys. B, 30, 1
Badnell, N. R., O'Mullane, M., Summers, H. P., et al. 2003, A&A, 406, 1151 (Paper I)
Badnell, N. R., & Pindzola, M. S. 1989, Phys. Rev. A, 39, 1685
Badnell, N. R., Pindzola, M. S., Dickson, W. J., et al. 1993, ApJ, 407, L91
Bartsch, T., Müller, A., Spies, W., et al. 1997, Phys. Rev. Lett., 79, 2233
Böhm, S., Müller, A., Schippers, S., et al. 2003, A&A, 405, 1157
Böhm, S., Schippers, S., Shi, W., et al. 2002, Phys. Rev. A, 65, 052728
Chen, M. H. 1991, Phys. Rev. A, 44, 4215
Colgan, J., Pindzola, M. S., Whiteford, A. W., & Badnell, N. R. 2003, A&A, 412, 597 (Paper III)
Dittner, P. F., Datz, S., Miller, P. D., Pepmiller, P. L., & Foux, C. M. 1987, Phys. Rev. A, 35, 3668
Glans, P., Lindroth, E., Badnell, N. R., et al. 2001, Phys. Rev. A, 64, 043609
Gorczyca, T. W., Robicheaux, F., Pindzola, M. S., & Badnell, N. R. 1996, Phys. Rev. A, 54, 2107
Griffin, D. C., Mitnik, D. M., Pindzola, M. S., & Robicheaux, F. 1998, Phys. Rev. A, 58, 4548
Griffin, D. C., & Pindzola, M. S. 1987, Phys. Rev. A, 35, 2821
Griffin, D. C., Pindzola, M. S., & Bottcher, C. 1985, Phys. Rev. A, 31, 568
Griffin, D. C., Pindzola, M. S., & Bottcher, C. 1985, Phys. Rev. A, 33, 3124
Griffin, D. C., Pindzola, M. S., & Krylstedt, P. 1989, Phys. Rev. A, 40, 6699
Griffin, D. C., Robicheaux, F., & Pindzola, M. S. 1998, Phys. Rev. A, 57, 2708
Gu, M. F. 2003, ApJ, 590, 1131
Kilgus, G., Hubs, D., Schwalm, D., et al. 1992, Phys. Rev. A, 46, 5730
Mannervik, S., DeWitt, D., Engström, L., et al. 1998, Phys. Rev. Lett., 81, 313
Mazzotta, P., Mazzitelli, G., Colafrancesco, S., & Vittorio, N. 1998, A&AS, 133, 403
Mitnik, D. M., Pindzola, M. S., & Badnell, N. R. 1999, Phys. Rev. A, 59, 3592
Pindzola, M. S., & Badnell, N. R. 1992, Nucl. Fusion and Plasma Material Interaction data for fusion, 3, 101
Pindzola, M. S., Badnell, N. R., & Griffin, D. C. 1992, Phys. Rev. A, 46, 5725
Savin, D. W. 2000, ApJ, 533, 106
Schennach, S., Müller, A., Uwira, O., et al. 1994, Z. Phys. D, 30, 291
Schippers, S., Bartsch, T., Bradnau, C., et al. 2000, Phys. Rev. A, 62, 022708
Schippers, S., Müller, A., Gwinner, G., et al. 2001, ApJ, 555, 1027
Summers, H. P. 2001, ADAS User Manual (2nd Edition), available from `http://adas.phys.strath.ac.uk/adas/docs/manual`
Tokman, M., Eklöw, N., Glans, P., et al. 2002, Phys. Rev. A, 66, 012703
Trefftz, E. J. 1969, in Physics of One and Two Electron Atoms, ed. F. Bopp, & H. Kleinpoppen (North-Holland, Amsterdam), 839
Zatsarinny, O., Gorczyca, T. W., Korista, K. T., Badnell, N. R., & Savin, D. W. 2003, A&A, 412, 587 (Paper II)
Zatsarinny, O., Gorczyca, T. W., Korista, K. T., Badnell, N. R., & Savin, D. W. 2004, A&A, 417, 1173 (Paper IV)
Zong, W., Schuch, R., Lindroth, E., et al. 1997, Phys. Rev. A, 56, 386